HHS Public Access

Author manuscript

ACS Chem Biol. Author manuscript; available in PMC 2022 June 18.

Published in final edited form as:

ACS Chem Biol. 2021 June 18; 16(6): 1050–1058. doi:10.1021/acschembio.1c00217.

Nematode Signaling Molecules Are Extensively Metabolized by Animals, Plants, and Microorganisms

Yan Yu[∇],
Boyce Thompson Institute and Department of Chemistry and Chemical Biology, Cornell University, Ithaca, New York 14853, United States

Ying K. Zhang[∇],
Boyce Thompson Institute and Department of Chemistry and Chemical Biology, Cornell University, Ithaca, New York 14853, United States

Murli Manohar,
Boyce Thompson Institute and Department of Chemistry and Chemical Biology, Cornell University, Ithaca, New York 14853, United States

Alexander B. Artyukhin,
Chemistry Department, College of Environmental Science and Forestry, State University of New York, Syracuse, New York 13210, United States

Anshu Kumari,
Boyce Thompson Institute, Cornell University, Ithaca, New York 14853, United States

Francisco J. Tenjo-Castano,
Boyce Thompson Institute, Cornell University, Ithaca, New York 14853, United States

Hung Nguyen,
Holoclara, Inc., Pasadena, California 91101, United States

Pratyush Routray,
Department of Chemistry and Chemical Biology, Cornell University, Ithaca, New York 14853, United States

Andrea Choe,
Holoclara, Inc., Pasadena, California 91101, United States

Daniel F. Klessig,

Corresponding Author: Frank C. Schroeder − Boyce Thompson Institute and Department of Chemistry and Chemical Biology, Cornell University, Ithaca, New York 14853, United States; schroeder@cornell.edu.

Author Contributions

All authors contributed to experimental design and data analysis. Y.K.Z. and A.B.A. synthesized and purified ascarosides. F.C.S. and Y.Y. wrote the manuscript.

[∇]These authors contributed equally to this work.

ASSOCIATED CONTENT

Supporting Information

The Supporting Information is available free of charge at https://pubs.acs.org/doi/10.1021/acschembio.1c00217.

General methods, ascaroside treatment procedures, methods for mass spectrometric analyses, synthetic procedures with NMR spectroscopic data, Figures S1–S9, Table S1, and NMR spectra (PDF)

The authors declare the following competing financial interest(s): Andrea Choe and Frank Schroeder are co-founders of Holoclara, Inc., and Frank Schroeder and Murli Manohar are co-founders of Ascribe Bioscience, Inc.

Boyce Thompson Institute, Cornell University, Ithaca, New York 14853, United States

Frank C. Schroeder
Boyce Thompson Institute and Department of Chemistry and Chemical Biology, Cornell University, Ithaca, New York 14853, United States

Abstract

Many bacterivorous and parasitic nematodes secrete signaling molecules called ascarosides that play a central role regulating their behavior and development. Combining stable-isotope labeling and mass spectrometry-based comparative metabolomics, here we show that ascarosides are taken up from the environment and metabolized by a wide range of phyla, including plants, fungi, bacteria, and mammals, as well as nematodes. In most tested eukaryotes and some bacteria, ascarosides are metabolized into derivatives with shortened fatty acid side chains, analogous to ascaroside biosynthesis in nematodes. In plants and *C. elegans*, labeled ascarosides were additionally integrated into larger, modular metabolites, and use of different ascaroside stereoisomers revealed the stereospecificity of their biosynthesis. The finding that nematodes extensively metabolize ascarosides taken up from the environment suggests that pheromone editing may play a role in conspecific and interspecific interactions. Moreover, our results indicate that plants, animals, and microorganisms may interact with associated nematodes via manipulation of ascaroside signaling.

Graphical Abstract

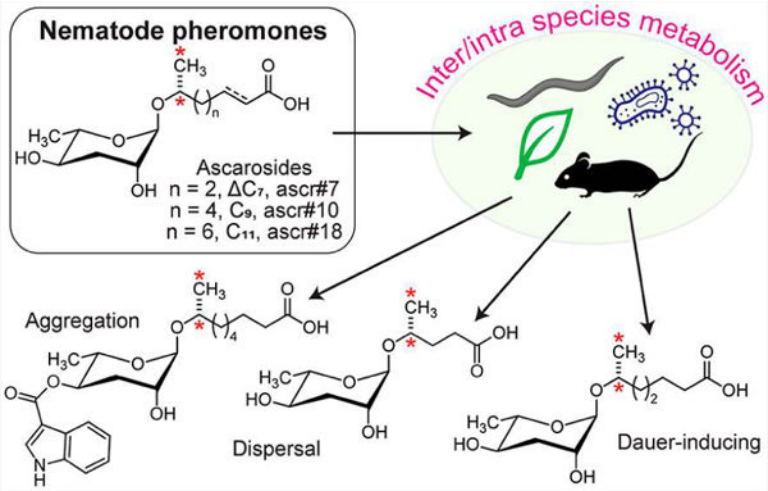

INTRODUCTION

Nematodes are the most abundant animals on Earth and participate in a wide range of ecological interactions.[1] Life cycles of nematodes are often highly complex, involving parasitic, pathogenic, and/or bacterivorous life stages. Correspondingly, nematodes interact intimately with diverse plants, animals, and microorganisms, and the ability to perceive and respond to the presence of nematodes appears likely to confer significant advantages to nematode-interacting species. A recent study showed that plants can sense low

nanomolar concentrations of nematode-derived pheromones called ascarosides and respond by upregulating specific defense signaling pathways.[2,3] Ascarosides were first shown to serve as signaling molecules in the model organism *C. elegans*, where they serve as a population density signal triggering larval diapause ("dauer").[4,5] Subsequent studies showed that ascarosides are used as signaling molecules also by many plant- and animal-parasitic nematodes.[2,6–9] In fact, ascarosides may be produced by a majority of nematode species, based on the results of targeted analyses of phylogenetically diverse species. Their biological functions range from regulating development, metabolism, and lifespan to coordinating social and mating behaviors.[10–13]

Ascarosides minimally consist of the dideoxyhexose ascarylose attached to a hydroxylated short-chain alkyl or alkenyl chain, as in the *C. elegans* dauer pheromone components ascr#2 (**1**) and ascr#3 (**2**). The fatty acid-like side chains originate from peroxisomal β-oxidation (pβo).[14,15] Such "simple" ascarosides serve as scaffolds for more-complex metabolites derived from attachment of diverse metabolic building blocks via carboxylesterases,[16,17] for example, icas#3 (**3**),[13] ascr#8 (**4**),[18] or uglas#1 (**5**) (see Figure 1a).[19] Ascarosides essentially function as a chemical language, and even small changes in the chemical structures of the ascarosides strongly affect biological activity. Correspondingly ascaroside biosynthesis is often specific to the sex or life stage. For example, the monounsaturated ascr#3 (**2**), which is produced primarily by *C. elegans* hermaphrodites, can extend the lifespan of *C. elegans*, whereas the saturated ascaroside ascr#10 (**6**), which is the most abundant ascaroside in *C. elegans* males, shortens lifespan[20] (Figure 1a). Although the biosyntheses of complex multimodular ascarosides or stereo-chemical variants is often species-specific, production of a few simple ascarosides is widespread among nematodes. For example, ascr#18 is produced by many plant parasitic and entomopathogenic nematodes, as well as most bacterivorous nematodes,[2] similarly ascr#1 is widespread among animal parasitic nematodes and bacterivorous species,[6,21] suggesting the possibility of interspecies signaling.

Recent studies indicate that a wide range of plant species, including monocots and dicots, as well as some fungi can perceive and respond to low concentrations of ascr#1 or ascr#18, indicating that plants and fungi evolved the ability to recognize ascarosides as a conserved molecular signature of nematodes.[2,22,23] Intriguingly, plants can metabolize nematode-derived ascarosides via pβo and thereby change their chemical message, generating ascaroside mixtures that repel plant-parasitic nematodes and reduce infection.[3] These findings suggest that ascaroside metabolism may play important roles in interphylum and intraphylum interactions involving nematodes, for example, in interactions with the host in the case of parasitic nematodes, or, in the case of bacterivorous and fungivorous nematodes, in the soil as part of a complex ecological network with bacteria, fungi, and plants. In this study, we aimed to investigate to what extent nematodes and nematode-interacting phyla can edit ascaroside pheromones taken up from their environment to potentially manipulate or interfere with nematode communication.

RESULTS AND DISCUSSION

Analytical Strategy.

We aimed to survey ascaroside metabolism across phyla in a strictly untargeted manner, avoiding *a priori* bias by knowledge of previously identified ascaroside derivatives and stereoisomers. For this purpose, we designed a set of stable-isotope labeled ascarosides that would enable unambiguous recognition of derivatives via comparative metabolomics and distinguishing metabolites derived from exogenously applied ascarosides from endogenously produced ascaroside derivatives (Figures 1b and 1c). Design of isotopically labeled ascarosides further aimed to ensure facile detection of labeled metabolites by comparative metabolomics software (e.g., XCMS[24] or MZmine 2[25]). Carbon-13 was selected over deuterium to avoid retention time shifts that could interfere with automated peak recognition, and a mass difference of 2 amu was deemed sufficient to distinguish natural isotopes from metabolites of added labeled synthetic compounds. The label had to be incorporated at a position in the ascarosides that is unlikely to be lost by known metabolic transformations, e.g., pβo, which has been shown to iteratively shorten the fatty acid-like side chains of ascarosides in nematodes[14,15,26] and plants.[3] Furthermore, synthesis of labeled ascarosides with a range of side chain lengths seemed useful, since in nematodes, ascarosides with different side chain lengths appear to have different metabolic fates.[27] Lastly, in order to test whether there is any preference or specificity for metabolism of the naturally occurring ascarosides, we aimed for a synthesis that would also allow for preparation of ascarosides with inverted configuration (*S* instead of *R*) in the side chain, which had not been described from natural sources.[10]

Synthesis of [$^{13}C_2$]-Ascarosides.

Based on these considerations, we opted for label incorporation at the ω and $\omega-1$ positions of the ascaroside side chain (see Figure 1c). [$^{13}C_2$]-labeled acetyl chloride was converted into the Weinreb amide and chain extended to near-racemic [$^{13}C_2$]-labeled 5-hexen-2-ol, which was then coupled to bis-benzoyl protected ascarylose.[28] The resulting mixture of stereoisomers (**7**) was subjected to metathesis with ethyl acrylate followed by deprotection, and chromatographic separation of the stereoisomers, which yielded pure samples of [$^{13}C_2$]-ascr#7 (**8**) as well as the [$^{13}C_2$]-(6*S*)-isomer (**9**). In previous work, we have shown that metathesis of **7** with longer chained terminally unsaturated fatty acid esters produces a mixture of products with different side chains, because of double bond migration and participation of the initial products in additional metathesis.[29] Though a nuisance in the earlier study, we took advantage of metathesis chain walking here by reacting 7 with ethyl-6-heptenoate, which produced a mixture of [$^{13}C_2$]-labeled ascarosides with side chain lengths of 9–12 carbons, Chromatographic separation afforded pure samples of ascr#10 and ascr#18, as well as their ($\omega-1$ *S*)-isomers (see Figure 1c).

Metabolism in *C. elegans*.

To investigate metabolism of exogenously supplied ascarosides in nematodes, we treated *C. elegans* wild-type cultures in parallel with [$^{13}C_2$]-labeled or nonlabeled ascarosides at 10 μM, a nontoxic concentration at the upper end of the range of ascaroside concentrations typically used for bioassays with *C. elegans*. For comparative HPLC-HRMS analysis of

treated and mock-treated cultures, we used Metaboseek software, which integrates the XCMS platform (Figure 1b).[24] Analysis of worms treated with [$^{13}C_2$]-labeled samples of ascr#7 (ΔC7, **8**), ascr#10 (C9, **10**) and ascr#18 (C11, **11**), all of which are naturally excreted by *C. elegans*,[14] revealed 24 [$^{13}C_2$]-labeled metabolites (see Figures 2a and 2b, as well as Figure S1 in the Supporting Information (SI)). [$^{13}C_2$]-ascr#10 and [$^{13}C_2$]-ascr#18 were converted to the corresponding β-hydroxylated derivatives and underwent side chain shortening, likely via pβo, resulting in the formation of [$^{13}C_2$]-ascr#9 (C5, **12**), the known end point of pβo of (ω−1)-ascarosides in *C. elegans*.[14] In contrast, treatment with [$^{13}C_2$]-ascr#7 (ΔC7) produced only trace quantities of $^{13}C_2$-ascr#9 (C5) and other pβo intermediates (see Figure 2b, as well as Figure S2 in the SI).

All three [$^{13}C_2$]-labeled ascarosides further contributed to the biosynthesis of modular ascarosides. [$^{13}C_2$]-ascr#10 and [$^{13}C_2$]-ascr#18 were predominantly incorporated into several 4′-modified ascarosides, e.g., icas#10 (**13**) and icas#18 (**14**), whereas [$^{13}C_2$]-ascr#7 was predominantly incorporated into compounds resulting from the attachment of additional moieties to the carboxy terminus, e.g., ascr#81 (**15**) and iglas#71 (**16**) (Figures 2a and 2b, as well as Figure S1). In addition, all three [$^{13}C_2$]-ascarosides were converted to corresponding phosphorylated ascarosides, e.g., phascr#181 (**17**).[30] Notably, [$^{13}C_2$]-ascr#10 was not significantly incorporated into osas#10, a 4′-modified derivative bearing succinyl octopamine moiety, suggesting that the biosynthesis of osas#10 and other succinyl octopamine modified ascarosides is distinct from that of other 4′-modified ascarosides, such as icas#10 (**13**) (see Figure 2c, as well as Figure S2). Separate biosyntheses of these signaling molecules would parallel their starkly different biological functions: osas#10 and its chain-shortened derivative osas#9 serve as dispersal signals,[31] whereas icas ascarosides promote aggregation.[13,14]

Untargeted comparative metabolomics further revealed incorporation of [$^{13}C_2$]-ascr#10 and [$^{13}C_2$]-ascr#18 into a series of amino acids conjugates,[30] as well as previously unreported cadaverine (ascad#10, **18**) and glycerol derivatives (see Figures 2a, 2d, and 2e, as well as Figure S1). These structures were proposed based on high-resolution MS fragmentation patterns and have been subsequently confirmed via synthesis for the case of ascad#10 (see Figure 2d, as well as Figure S3 in the SI). Notably, amino acid conjugates of [$^{13}C_2$]-ascr#18 (C11) were much more abundant than the corresponding ascr#10 (C9) conjugates, and corresponding ascr#7 (ΔC7) conjugates were not observed (see Figures 2b and 2e). Among amino acids conjugates, the alanine, valine, glutamate, and glutamine derivatives were most abundant, whereas glycine conjugates were not detected (Figure 2e), in contrast to *acox-1.1* null mutants, which endogenously accumulate ascr#10 and ascr#18 and produce the corresponding glycine derivatives as the most abundant amino acid conjugates.[30] These observations suggest that exogenous ascarosides taken up from the environment are metabolized differently than endogenously produced ascarosides.

Next, we tested whether stereoisomers of [$^{13}C_2$]-ascr#7, [$^{13}C_2$]-ascr#10, and [$^{13}C_2$]-ascr#18 carrying (*S*)-configuration at the (ω−1)-position of the side chain are similarly metabolized. Although the (*S*)-stereoisomers were taken up by *C. elegans* to a similar extent as the (*R*)-stereoisomers, they were less extensively metabolized (Figure 2a). We did not observe any conversion to 4′-modified ascarosides, and conjugation with additional moieties at

the carboxy terminus was partially abolished, e.g., (*S*)-[$^{13}C_2$]-ascr#7 was not converted to (*S*)-[$^{13}C_2$]-ascr#81 and (*S*)-[$^{13}C_2$]-iglas#71, whereas formation of the closely related iglas#91 and of C-terminal conjugates with cadaverine, e.g., ascad#10 (**18**), was not affected (see Figure 2a, as well as Figure S4 in the SI). In contrast, the $^{13}C_2$-labeled (*S*)-stereoisomers were phosphorylated, conjugated with amino acids, and chain-shortened via p*β*o, resulting in formation of (*S*)-[$^{13}C_2$]-ascr#9 (**19**), as confirmed through independent synthesis (see Figures 2a and 2f, as well as Figure S5 in the SI).

Following the identification of (*S*)-ascr#9 as the most abundant metabolite of side-chain (*S*)-configured ascarosides, we noted the presence of small amounts of this compound in *exo*- and *endo*-metabolome samples from untreated *C. elegans* (see Figures 2f and 2g, as well as Figure S5 in the SI). This was unexpected, since all previously identified (*ω*−1)-ascarosides are (*R*)-configured.[10] However, reinspection of previously published HPLC-MS data[27] revealed that (*S*)-ascr#9 can be detected consistently in *C. elegans* metabolome samples, albeit in variable amounts. Production of (*S*)-ascr#9 appears to be increased in worms grown on plates compared to liquid culture, and is *daf-22*-dependent, indicating that (*S*)-ascr#9, analogous to the (*R*)-isomer, originates from chain shortening of long-chain (*S*)-ascarosides (Figure 2g).

Metabolism in Microorganisms.

Bacterivorous and fungivorous nematodes are among the most abundant animals in soil, where they feed on and interact with complex microbiomes. Moreover, *C. elegans* and other bacterivorous nematodes are commonly raised on bacterial diets in the lab; however, whether bacterial metabolism interacts with pheromone signaling has remained unclear.[32] To investigate potential metabolism of ascarosides by microorganisms, we treated a soil fungus, *A. fumigatus*, the yeast *S. cerevisiae*, and three different bacteria (*Bacillus subtilis*, *Pseudomonas syringae*, and *Escherichia coli* OP50), which is commonly used as food for *C. elegans* in the laboratory, with [$^{13}C_2$]-labeled or unlabeled ascr#18 (C11, **16**). Comparative metabolomic analysis after 24 h revealed that, in *A. fumigatus*, ascr#18 is rapidly taken up and converted to the chain-shortened derivatives ascr#1 (C7, **20**) and ascr#9 (C5, **12**), indicating that *A. fumigatus* takes up ascr#18 and metabolizes the compound via *β*-oxidation, as in ascaroside biosynthesis in nematodes,[14] and analogous to the metabolism of ascarosides in plants[3] (see Figures 3a and 3b, as well as Figure S6a in the SI). In contrast, analysis of ascr#18-treated *S. cerevisiae* revealed only a small amount of ascr#18 uptake, and no chain shortening or other metabolites were detected, except for trace amounts of a glycosylated derivative of ascr#18 (see Figure 3b, as well as Figure S6b in the SI), which was found to be identical to the glucoside glas#18 (**21**) previously reported from *C. elegans*.[14]

Analysis of ascr#18-treated *P. syringae* revealed iterative side chain shortening suggestive of *β*-oxidation (Figure 3c); however, compared to *A. fumigatus*, ascr#18 metabolism in *P. syringae* proceeded much slower and produced mostly ascr#10 (C9, **6**), whereas in *A. fumigatus* and plant *β*-oxidation proceeds further, yielding ascr#9 (C5, **12**) as the most abundant metabolite[3]. Notably, analysis of the *P. syringae endo*-metabolome (the extract of the bacterial pellet) revealed only trace amounts of ascarosides, suggesting that any ascr#18

taken up is metabolized relatively quickly and then excreted (see Figure 3c, as well as Figure S6c in the SI). In contrast, ascr#18 was not metabolized in *B. subtilis* or *E. coli* OP50 (see Figure 3c, as well as Figure S6d in the SI).

Metabolism in Mammals.

Nematodes are common parasites of plants and animals, including humans,[33] and both plant and animal parasitic nematodes have been shown to produce ascarosides.[2,6] To investigate potential metabolism of ascarosides in mammals, we first treated human hepatocytes with [$^{13}C_2$]-labeled and unlabeled ascr#7 (ΔC7, **22**). Comparative metabolomic analysis revealed chain shortening to ascr#9 in human cells within 2 h (see Figures 3d and 3e, as well as Figure S7a in the SI), likely from β-oxidation, following activation by an acyl-CoA synthetase. In addition, we detected small amounts of the saturated derivative of ascr#7, ascr#1 (**20**), which suggests that ascr#7 may be reduced by peroxisomal or mitochondrial enoyl reductases (see Figures 3d and 3e, as well as Figure S7a). Next, we investigated ascaroside metabolism *in vivo* in mice and rats. Mice metabolized most intravenously (IV)-administered ascr#7 to ascr#9 within 20 min. In the case of oral (PO) administration, ascr#7 was absorbed into the bloodstream within <0.5 h and then was metabolized to ascr#9, reaching peak ascr#9 concentrations after 1 h (see Figure 3f). As in human cell culture, we additionally observed formation of small amounts of ascr#1 as well as trace quantities of bhas#1 (**23**), likely derived from the hydration of ascr#7 by the peroxisomal enoyl-CoA hydratase (see Figure 3d, as well as Figures S7b and S7c in the SI). Both ascr#7 and ascr#9 were largely cleared from the bloodstream after 8 h, suggesting that it was eliminated via feces or urine or stored in, e.g., fat tissue. To assess routes of elimination, we conducted additional analyses in rats. Analysis of rat serum and urine samples confirmed rapid metabolism of PO- or IV-administered ascr#7 into ascr#9, which was excreted in the urine after 8−24 h. Analysis of fecal samples of PO-treated animals additionally revealed unmetabolized ascr#7, in addition to smaller amounts of ascr#9 (Figures S7d, S7e, S7f, and S7g in the SI). Given that chain shortening of ascarosides proceeds via pβo in nematodes and plants, we hypothesize that chain shortening of ascarosides in mammals similarly relies on peroxisomal fatty acid metabolism.

Metabolism in Plants.

In a previous study, we showed that both monocots and dicots metabolize ascr#18 via pβo into ascarosides with shorter side chains, e.g., ascr#9.[3] To more broadly investigate metabolism of ascarosides in plants, we treated *Arabidopsis* (*Brassicaceae*) and tomato (*Solanaceae*) seedlings with [$^{13}C_2$]-labeled or unlabeled ascr#18 (C11, **16**). As expected, comparative metabolomic analysis after 24 h showed that ascr#18 is iteratively chain-shortened in both *Arabidopsis* and tomato, resulting in the conversion of most of the free ascr#18 to ascr#9 (C5, **12**) (see Figures 4a and 4b, as well as Figure S8 in the SI). In addition, we detected several series of glycosylated derivatives, derived from conjugation of ascr#18 and chain-shortened ascarosides with one or more hexose units (see Figure 4a, as well as Figure S7). Comparison of MS^2 fragmentation patterns and retention times indicated that glycosylated derivatives detected in *Arabidopsis* and tomato are identical to glucosylated ascarosides previously reported from *C. elegans*, e.g., glas#18 (**21**) (see Figures S8 and S9 in the SI). Glucosylated ascarosides were much more abundantly produced

in tomato, where we additionally detected ascr#18 derivatives incorporating two or three hexose moieties, which are absent in *Arabidopsis* (Figure 4b). In turn, *Arabidopsis* produced a glutamate conjugate (**25**) of ascr#18, which was not detected in tomato (see Figures 4a and 4b, as well as Figure S8 in the SI). Taken together, our observation indicated that ascarosides are taken up and metabolized by plants via pβo, glycosylation, and amino acid conjugation pathways, producing a range of metabolites, many of which are also found in the metabolomes of *C. elegans* and other nematodes (Figure 4c).

DISCUSSION

Our results indicate that the capacity to metabolize ascarosides is widely conserved among nematode-interacting phyla, suggesting that nematode-associated plants, animals, and microorganisms may interact in part via manipulation of ascaroside signaling. Given that even seemingly minor changes in ascaroside structures[20] or the composition of ascaroside blends[3,34] can be associated with stark changes in signaling content, this xenometabolic activity of nematode-associated microbiota and macrobiota may play a significant role in nematode ecology, e.g., in the context of host-parasite interaction or in the soil where nematodes interact closely with diverse arthropods and microorganisms.[35] Metabolism of ascarosides by microorganisms or by host plants or animals may also confer information to the producing nematodes, e.g., about the suitability of soil environments for colonization or of hosts for invasion, respectively.

Metabolism of nematode-secreted ascarosides by associated microbiota and macrobiota can change the composition of pheromone blends rapidly, at time scales of a few hours or less, and thus has the potential to confound studies of pheromone signaling in *C. elegans* and other nematode species. Therefore, bioassays, e.g., using synthetic ascarosides, must take xenometabolic effects into account, including the possibility that nematodes themselves further edit pheromone blends. In *C. elegans*, comparative analysis of samples treated with or without isotopically labeled compounds allowed to distinguish native ascaroside metabolism and showed that exogenously supplied ascarosides were chain-shortened, converted to phosphorylated derivatives, and integrated into structurally more-complex modular ascarosides in a stereoselective and side chain-specific manner. Even though only a fraction of a percent of added ascaroside was converted to any one type of modular metabolite, the resulting changes in ascaroside bouquets may significantly affect nematode responses, given that biological activities may be dependent on the relative ratios of ascaroside abundances[34] and since modular ascarosides are often active at subnanomolar concentrations.[13,14,20] For example, the ratio of ascr#3 to ascr#10 is critical for behavioral and physiological responses of *C. elegans* hermaphrodites and males,[20,34] and in the case of plant parasitic nematodes, juveniles are attracted by ascr#18, but repulsed by mixtures of ascr#18 and ascr#9.[3] Further editing of supplied synthetic ascarosides may also warrant consideration when comparing pheromone responses of wildtype with worms defective in peroxisomal β-oxidation, e.g., *daf-22* mutants,[14,18,26] which have been used as a control for worms lacking endogenously produced ascarosides in a large number of studies with synthetic ascarosides.[36–38]

Behavioral responses to ascarosides have so far been studied only in a small number of nematode species,[10] and the activities of complex blends of compounds have been explored only to a very limited extent. Even in the model systems *C. elegans* and *P. pacificus*, the biological functions of ascr#9, the proximal endproduct of ascaroside metabolism in most of the eukaryotes studied here has not been extensively tested. Our results may motivate a survey of responses to ascr#9 in nematodes from diverse ecological niches. Lastly, treatment of *C. elegans* with (*S*)-ascarosides led to the unexpected identification of an ascaroside with inverted side-chain stereochemistry in untreated *C. elegans*, which highlights gaps in our understanding of ascaroside biosynthesis and will further motivate more comprehensive characterization of responses to different ascaroside blends and stereoisomers. Moreover, it is unclear whether perception of exogenous ascarosides influences their uptake and metabolism or the biosynthesis and excretion of endogenous ascarosides. This question could potentially be addressed by investigating ascaroside metabolism and biosynthesis in mutants defective in ascaroside perception.[10]

Extensive metabolism of excreted signaling molecules by conspecifics or associated microbiota and macrobiota is not restricted to nematode-derived ascarosides. Examples for the degradation of pheromones by conspecific are well-known from insects, e.g., the silkmoth.[39] A classic example for the role of microbiota in processing signaling molecules in higher animals is the metabolism of excreted primary bile acids by intestinal bacteria, resulting in the formation of secondary bile acids, which are then reabsorbed and regulate diverse aspects of host metabolism and immune function.[40,41] We believe that editing of small molecule signals by conspecifics, other animals, plants, and associated microorganisms may be widespread and represent an underappreciated regulatory mechanism in ecological networks.

METHODS

For detailed experimental and synthetic procedures, see the Supporting Information.

Supplementary Material

Refer to Web version on PubMed Central for supplementary material.

ACKNOWLEDGMENTS

This research was supported in part by National Institutes of Health Grant Nos. R01GM113692 and R01GM088290 (to F.C.S.). F.C.S. is a Faculty Scholar of the Howard Hughes Medical Institute. We thank WormBase for sequences, N. Movahed for assistance with mass spectrometry, and D. Kiemle for assistance with NMR spectroscopy.

REFERENCES

(1). van den Hoogen J, Geisen S, Routh D, Ferris H, Traunspurger W, Wardle DA, de Goede RGM, Adams BJ, Ahmad W, Andriuzzi WS, Bardgett RD, Bonkowski M, Campos-Herrera R, Cares JE, Caruso T, de Brito Caixeta L, Chen X, Costa SR, Creamer R, Mauro da Cunha Castro J, Dam M, Djigal D, Escuer M, Griffiths BS, Gutiérrez C, Hohberg K, Kalinkina D, Kardol P, Kergunteuil A, Korthals G, Krashevska V, Kudrin AA, Li Q, Liang W, Magilton M, Marais M, Martín JAR, Matveeva E, Mayad EH, Mulder C, Mullin P, Neilson R, Nguyen TAD, Nielsen UN, Okada H, Rius JEP, Pan K, Peneva V, Pellissier L, Carlos Pereira da Silva J, Pitteloud C, Powers

TO, Powers K, Quist CW, Rasmann S, Moreno SS, Scheu S, Setälä H, Sushchuk A, Tiunov AV, Trap J, van der Putten W, Vestergaard M, Villenave C, Waeyenberge L, Wall DH, Wilschut R, Wright DG, Yang JI, and Crowther TW (2019) Soil nematode abundance and functional group composition at a global scale. Nature 572, 194–198. [PubMed: 31341281]

(2). Manosalva P, Manohar M, von Reuss SH, Chen S, Koch A, Kaplan F, Choe A, Micikas RJ, Wang X, Kogel KH, Sternberg PW, Williamson VM, Schroeder FC, and Klessig DF (2015) Conserved nematode signalling molecules elicit plant defenses and pathogen resistance. Nat. Commun 6, 7795. [PubMed: 26203561]

(3). Manohar M, Tenjo-Castano F, Chen S, Zhang YK, Kumari A, Williamson VM, Wang X, Klessig DF, and Schroeder FC (2020) Plant metabolism of nematode pheromones mediates plant-nematode interactions. Nat. Commun 11, 208. [PubMed: 31924834]

(4). Jeong PY, Jung M, Yim YH, Kim H, Park M, Hong E, Lee W, Kim YH, Kim K, and Paik YK (2005) Chemical structure and biological activity of the *Caenorhabditis elegans* dauer-inducing pheromone. Nature 433, 541–545. [PubMed: 15690045]

(5). Butcher RA, Fujita M, Schroeder FC, and Clardy J (2007) Small-molecule pheromones that control dauer development in Caenorhabditis elegans. Nat. Chem. Biol 3, 420–422. [PubMed: 17558398]

(6). Choe A, von Reuss SH, Kogan D, Gasser RB, Platzer EG, Schroeder FC, and Sternberg PW (2012) Ascaroside signaling is widely conserved among nematodes. Curr. Biol 22, 772–780. [PubMed: 22503501]

(7). Noguez JH, Conner ES, Zhou Y, Ciche TA, Ragains JR, and Butcher RA (2012) A novel ascaroside controls the parasitic life cycle of the entomopathogenic nematode *Heterorhabditis bacteriophora*. ACS Chem. Biol 7, 961–966. [PubMed: 22444073]

(8). Yim JJ, Bose N, Meyer JM, Sommer RJ, and Schroeder FC (2015) Nematode signaling molecules derived from multimodular assembly of primary metabolic building blocks. Org. Lett 17, 1648–1651. [PubMed: 25782998]

(9). Bose N, Ogawa A, von Reuss SH, Yim JJ, Ragsdale EJ, Sommer RJ, and Schroeder FC (2012) Complex small-molecule architectures regulate phenotypic plasticity in a nematode. Angew. Chem., Int. Ed 51, 12438–12443.

(10). von Reuss SH (2018) Exploring Modular Glycolipids Involved in Nematode Chemical Communication. Chimia 72, 297–303. [PubMed: 29789066]

(11). von Reuss SH, and Schroeder FC (2015) Combinatorial chemistry in nematodes: modular assembly of primary metabolism-derived building blocks. Nat. Prod. Rep 32, 994–1006. [PubMed: 26059053]

(12). Butcher RA (2017) Small-molecule pheromones and hormones controlling nematode development. Nat. Chem. Biol 13, 577–586. [PubMed: 28514418]

(13). Srinivasan J, von Reuss SH, Bose N, Zaslaver A, Mahanti P, Ho MC, O'Doherty OG, Edison AS, Sternberg PW, and Schroeder FC (2012) A modular library of small molecule signals regulates social behaviors in *Caenorhabditis elegans*. PLoS Biol 10, No. e1001237. [PubMed: 22253572]

(14). von Reuss SH, Bose N, Srinivasan J, Yim JJ, Judkins JC, Sternberg PW, and Schroeder FC (2012) Comparative metabolomics reveals biogenesis of ascarosides, a modular library of small-molecule signals in *C. elegans*. J. Am. Chem. Soc 134, 1817–1824. [PubMed: 22239548]

(15). Zhang X, Feng L, Chinta S, Singh P, Wang Y, Nunnery JK, and Butcher RA (2015) Acyl-CoA oxidase complexes control the chemical message produced by *Caenorhabditis elegans*. Proc. Natl. Acad. Sci. U. S. A 112, 3955–3960. [PubMed: 25775534]

(16). Falcke JM, Bose N, Artyukhin AB, Rodelsperger C, Markov GV, Yim JJ, Grimm D, Claassen MH, Panda O, Baccile JA, Zhang YK, Le HH, Jolic D, Schroeder FC, and Sommer RJ (2018) Linking Genomic and Metabolomic Natural Variation Uncovers Nematode Pheromone Biosynthesis. Cell Chem. Biol 25, 787–796. [PubMed: 29779955]

(17). Le HH, Wrobel CJJ, Cohen SM, Yu J, Park H, Helf MJ, Curtis BJ, Kruempel JC, Rodrigues PR, Hu PJ, Sternberg PW, and Schroeder FC (2020) Modular metabolite assembly in *Caenorhabditis elegans* depends on carboxylesterases and formation of lysosome-related organelles. eLife 9, No. e61886. [PubMed: 33063667]

(18). Pungaliya C, Srinivasan J, Fox BW, Malik RU, Ludewig AH, Sternberg PW, and Schroeder FC (2009) A shortcut to identifying small molecule signals that regulate behavior and development in *Caenorhabditis elegans*. Proc. Natl. Acad. Sci. U. S. A 106, 7708–7713. [PubMed: 19346493]

(19). Curtis BJ, Kim LJ, Wrobel CJJ, Eagan JM, Smith RA, Burch JE, Le HH, Artyukhin AB, Nelson HM, and Schroeder FC (2020) Identification of Uric Acid Gluconucleoside-Ascaroside Conjugates in *Caenorhabditis elegans* by Combining Synthesis and MicroED. Org. Lett 22, 6724. [PubMed: 32820938]

(20). Ludewig AH, Artyukhin AB, Aprison EZ, Rodrigues PR, Pulido DC, Burkhardt RN, Panda O, Zhang YK, Gudibanda P, Ruvinsky I, and Schroeder FC (2019) An excreted small molecule promotes C. elegans reproductive development and aging. Nat. Chem. Biol 15, 838–845. [PubMed: 31320757]

(21). Choe A, Chuman T, von Reuss SH, Dossey AT, Yim JJ, Ajredini R, Kolawa AA, Kaplan F, Alborn HT, Teal PE, Schroeder FC, Sternberg PW, and Edison AS (2012) Sex-specific mating pheromones in the nematode *Panagrellus redivivus*. Proc. Natl. Acad. Sci. U. S. A 109, 20949–20954. [PubMed: 23213209]

(22). Hsueh YP, Gronquist MR, Schwarz EM, Nath RD, Lee CH, Gharib S, Schroeder FC, and Sternberg PW (2017) Nematophagous fungus Arthrobotrys oligospora mimics olfactory cues of sex and food to lure its nematode prey. eLife 6, 6.

(23). Hsueh YP, Mahanti P, Schroeder FC, and Sternberg PW (2013) Nematode-trapping fungi eavesdrop on nematode pheromones. Curr. Biol 23, 83–86. [PubMed: 23246407]

(24). Tautenhahn R, Bottcher C, and Neumann S (2008) Highly sensitive feature detection for high resolution LC/MS. BMC Bioinf 9, 504.

(25). Myers OD, Sumner SJ, Li S, Barnes S, and Du X (2017) Detailed Investigation and Comparison of the XCMS and MZmine 2 Chromatogram Construction and Chromatographic Peak Detection Methods for Preprocessing Mass Spectrometry Metabolomics Data. Anal. Chem 89, 8689–8695. [PubMed: 28752757]

(26). Markov GV, Meyer JM, Panda O, Artyukhin AB, Claaßen M, Witte H, Schroeder FC, and Sommer RJ (2016) Functional Conservation and Divergence of daf-22 Paralogs in *Pristionchus pacif icus* Dauer Development. Mol. Biol. Evol 33, 2506–2514. [PubMed: 27189572]

(27). Artyukhin AB, Zhang YK, Akagi AE, Panda O, Sternberg PW, and Schroeder FC (2018) Metabolomic “Dark Matter” Dependent on Peroxisomal beta-Oxidation in *Caenorhabditis elegans*. J. Am. Chem. Soc 140, 2841–2852. [PubMed: 29401383]

(28). Zhang YK, Sanchez-Ayala MA, Sternberg PW, Srinivasan J, and Schroeder FC (2017) Improved Synthesis for Modular Ascarosides Uncovers Biological Activity. Org. Lett 19, 2837–2840. [PubMed: 28513161]

(29). O’Doherty I, Yim JJ, Schmelz EA, and Schroeder FC (2011) Synthesis of caeliferins, elicitors of plant immune responses: accessing lipophilic natural products via cross metathesis. Org. Lett 13, 5900–5903. [PubMed: 21992613]

(30). Hoki JS, Le HH, Mellott KE, Zhang YK, Fox BW, Rodrigues PR, Yu Y, Helf MJ, Baccile JA, and Schroeder FC (2020) Deep Interrogation of Metabolism Using a Pathway-Targeted Click-Chemistry Approach. J. Am. Chem. Soc 142, 18449–18459. [PubMed: 33053303]

(31). Artyukhin AB, Yim JJ, Srinivasan J, Izrayelit Y, Bose N, von Reuss SH, Jo Y, Jordan JM, Baugh LR, Cheong M, Sternberg PW, Avery L, and Schroeder FC (2013) Succinylated octopamine ascarosides and a new pathway of biogenic amine metabolism in *Caenorhabditis elegans*. J. Biol. Chem 288, 18778–18783. [PubMed: 23689506]

(32). Darby C (2005) Interactions with microbial pathogens, In Worm Book, Ed.; The C. elegans Research Community, WormBook.

(33). Jasmer DP, Goverse A, and Smant G (2003) Parasitic nematode interactions with mammals and plants. Annu. Rev. Phytopathol 41, 245–270. [PubMed: 14527330]

(34). Aprison EZ, and Ruvinsky I (2017) Counteracting Ascarosides Act through Distinct Neurons to Determine the Sexual Identity of *C. elegans* Pheromones. Curr. Biol 27, 2589–2599. [PubMed: 28844646]

(35). Hsueh Y-P, Mahanti P, Schroeder FC, and Sternberg PW (2013) Nematode-Trapping Fungi Eavesdrop on Nematode Pheromones. Curr. Biol 23, 83–86. [PubMed: 23246407]

(36). Muirhead CS, and Srinivasan J (2020) Small molecule signals mediate social behaviors in *C. elegans*. J. Neurogenet 34, 395–403. [PubMed: 32990104]

(37). Wong SS, Yu J, Schroeder FC, and Kim DH (2020) Population Density Modulates the Duration of Reproduction of *C. elegans*. Curr. Biol 30, 2602–2607. [PubMed: 32442457]

(38). Park JY, Joo HJ, Park S, and Paik YK (2019) Ascaroside Pheromones: Chemical Biology and Pleiotropic Neuronal Functions. Int. J. Mol. Sci 20, 3898.

(39). Ishida Y, and Leal WS (2005) Rapid inactivation of a moth pheromone. Proc. Natl. Acad. Sci. U. S. A 102, 14075–14079. [PubMed: 16172410]

(40). Ramírez-Pérez O, Cruz-Ramón V, Chinchilla-López P, and Méndez-Sánchez N (2017) The Role of the Gut Microbiota in Bile Acid Metabolism. Ann. Hepatol 16, No. S21. [PubMed: 31196631]

(41). Ma C, Han M, Heinrich B, Fu Q, Zhang Q, Sandhu M, Agdashian D, Terabe M, Berzofsky JA, Fako V, Ritz T, Longerich T, Theriot CM, McCulloch JA, Roy S, Yuan W, Thovarai V, Sen SK, Ruchirawat M, Korangy F, Wang XW, Trinchieri G, and Greten TF (2018) Gut microbiome-mediated bile acid metabolism regulates liver cancer via NKT cells. Science 360, No. eaan5931. [PubMed: 29798856]

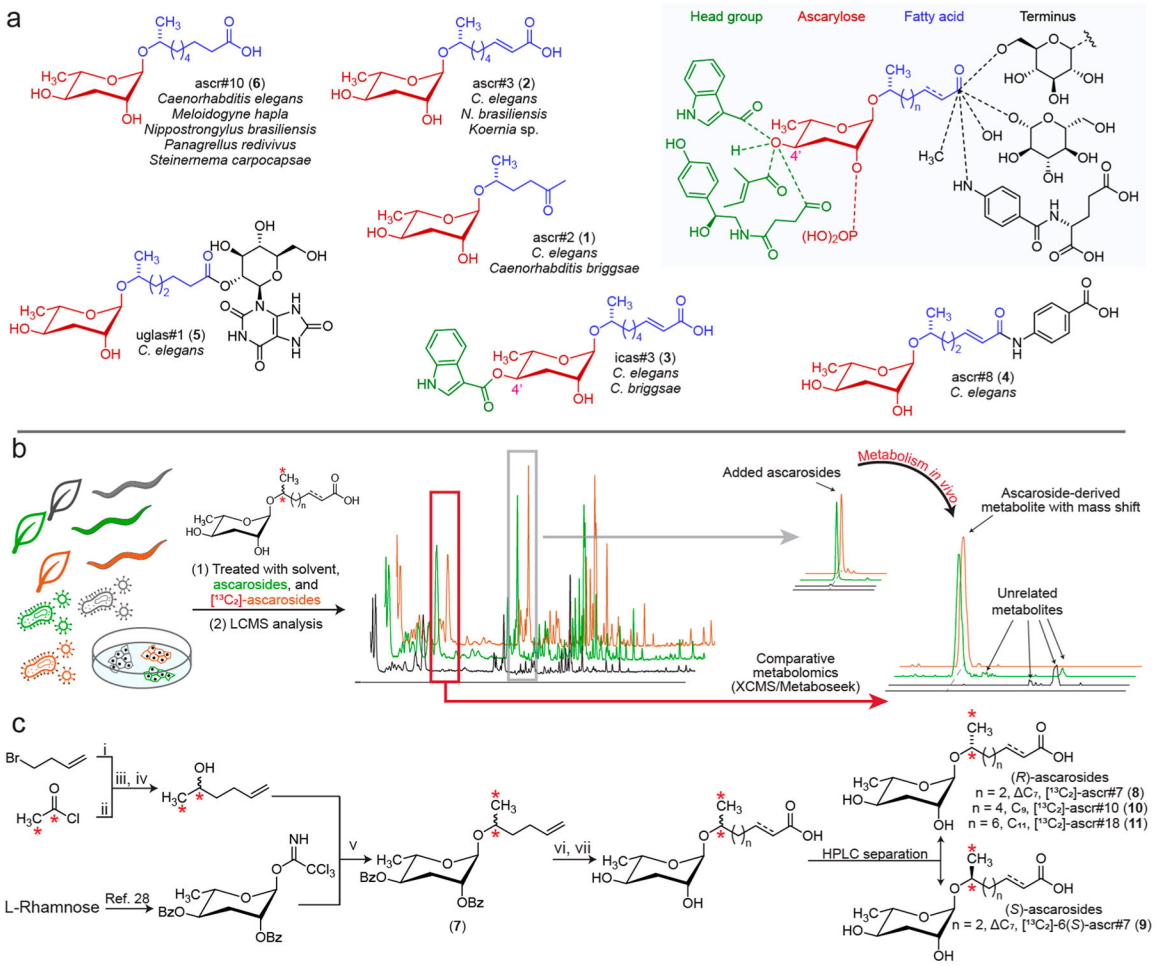

Figure 1.

Monitoring ascaroside metaboli in vivo. (a) Nematode-produced ascarosides are glycosides of the 3,6-dideoxysugar L-ascarylose (red) with an attached fatty acid-derived side chain (blue), which can be further decorated at the 4′ positions (green), or the C terminus (black). (b) Plants, *C. elegans*, microorganisms and mammalian cells were treated with control (black), ascarosides (green), and [$^{13}C_2$]-ascaroside (orange), followed by LCMS, XCMS, and comparative analysis. Metabolism of ascarosides were monitored by detecting differential peaks with a mass shift. (c) Synthesis route of different isotopically labeled (*R*)- and (*S*)-ascarosides: (i) Mg, ether, 1 h; (ii) CH_3NHOCH_3·HCl, TEA, DCM, 0 °C to RT, 3 h; (iii) ether, −20 to 0 °C, 4.5 h; (iv) Terashima reagent, ether, −78 °C, 30 min; (v) TMSOTf, DCM, 0 °C, 1 h; (vi) ethyl acrylate (ethyl 6-heptenoate), Grubb's 2nd catalyst, DCM, 4 h; and (vii) (Pd/C, H_2, EtOAc, 1 h), LiOH, dioxane, 60 °C 14 h.

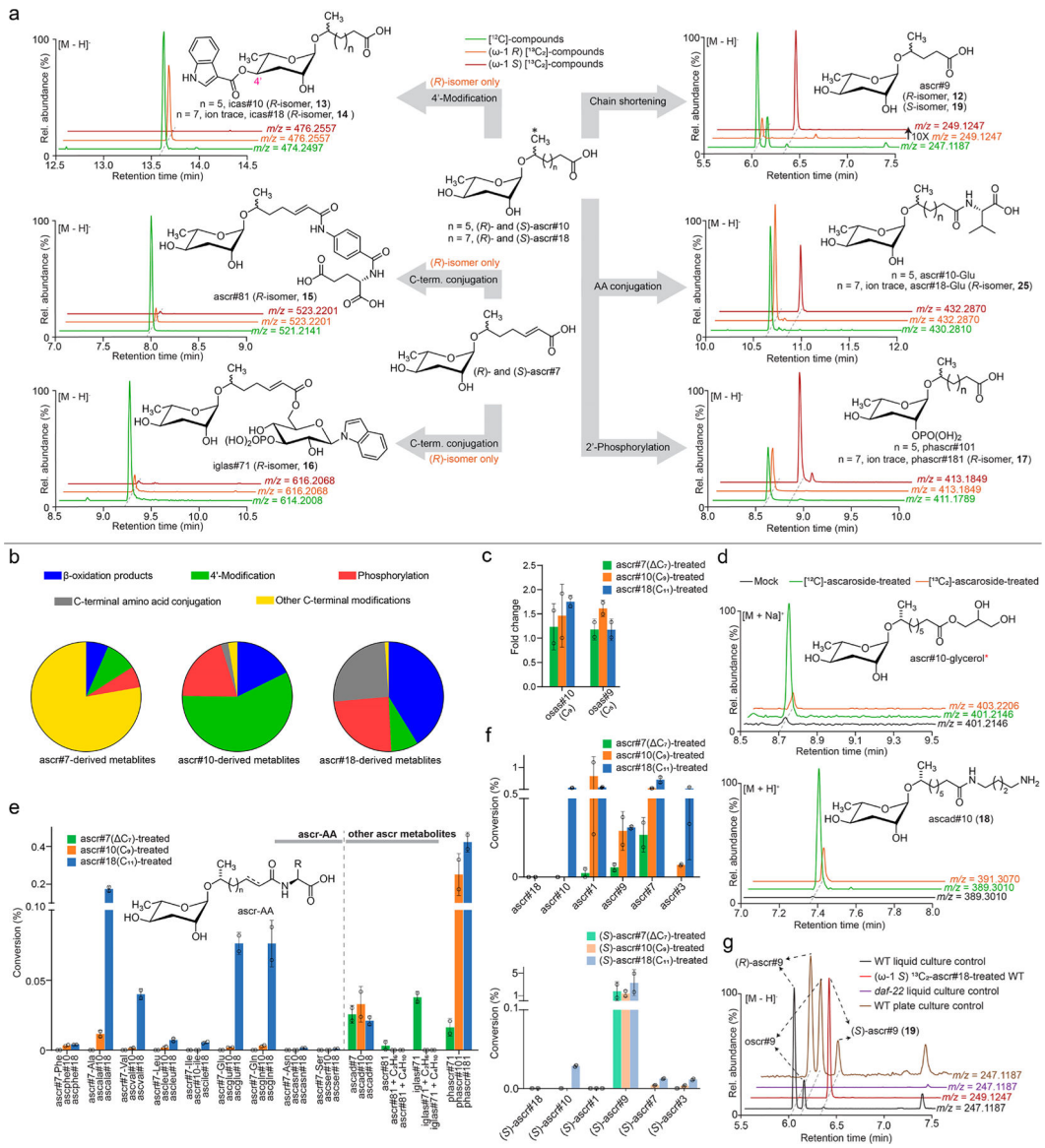

Figure 2.

C. elegans metabolism of exogenously supplied ascr#7, ascr#10, and ascr#18. (a) Major metabolic pathways of treated ascr#7, ascr#10, and ascr#18. Ion traces (ESI negative) of example ascaroside derivatives from treatments of ^{12}C-(*R*)-ascaroside (green), [$^{13}C_2$]-(*R*)-ascaroside (orange), and [$^{13}C_2$]-(*S*)-ascaroside (red). Arrows represent different metabolic pathways affected (*R*-isomer only) or not affected by the configuration of the side chain stereocenter. (b) Relative abundance of ascaroside-derived metabolites. (c) Fold change of $[M+2.006-H]^-$ for osas#10 and osas#9 by treating [$^{13}C_2$]-ascr#7, ascr#10, and ascr#18. (d) Examples of newly discovered ascarosides and representative ion chromatograms (ESI positive) from treatments with [$^{13}C_2$]-labeled ascarosides. (e) Conversion percentage of ascr#7 (green), ascr#10 (orange), and ascr#18 (blue) to the corresponding ascarosides-derived metabolites. Putative homologues of known ascarosides that were not detected are referred to as, e.g., "ascr#81+C_2H_6". (f) Conversion percentages of exogenously added (*S*)-

and (*R*)-ascr#7, ascr#10, and ascr#18 to different pβo products. Whereas pβo of added (*R*)-ascarosides produced a range of different chain lengths, the side chains of added (*S*)-ascarosides were shortened more quickly, yielding (*S*)-ascr#9 (C5) as the dominant product. (g) Ion chromatograms of (*R*)-ascr#9, oscr#9, and (*S*)-ascr#9 from endometabolomes of wild type grown in liquid (black), [$^{13}C_2$]-(*S*)-ascr#18-treated wild type grown in liquid, *daf-22* mutants grown in liquid (purple) and wildtype grown on plates (brown). Conversion percentages and compound distribution are calculated based on ratios of MS peak areas. Structures of compounds marked with an asterisk (*) were proposed based on MS^2 spectra and homology with known compounds.

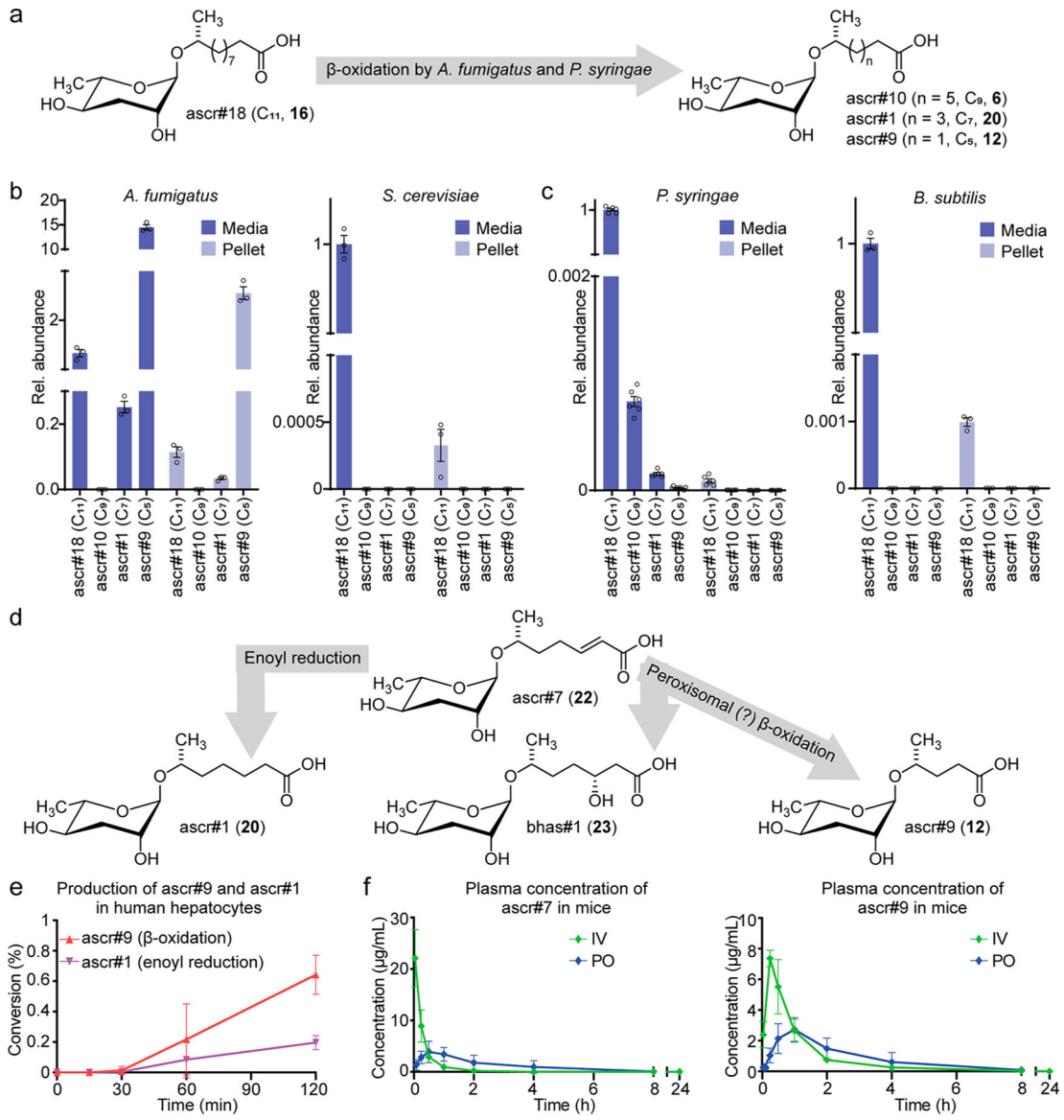

Figure 3.

Metabolism of ascr#18 in microorganisms, mammalian cells, and mammals. (a) ascr#18 is chain-shortened by *A. fumigatus* and *P. syringae* to ascr#10, ascr#1, and ascr#9; (b, c) relative abundance of ascr#18 and its chain-shortened products detected in the media (left) and pellet (right) by treatment of ascr#18 to *A. fumigatus* and *S. cerevisiae* (panel b) and *P. syringae* and *B. subtilis* (panel c). Metabolic pathways and products of ascr#7 in mice. (e) Abundance of ascr#9 (red) and ascr#1 (purple), relative to ascr#7 from the treatment of ascr#7 to human hepatocytes. (f) Plasma concentration of ascr#7 and ascr#9 in mice that received ascr#7 intravenously (IV, green) and orally (PO, blue) at concentrations of 50 and 100 mg/kg, respectively.

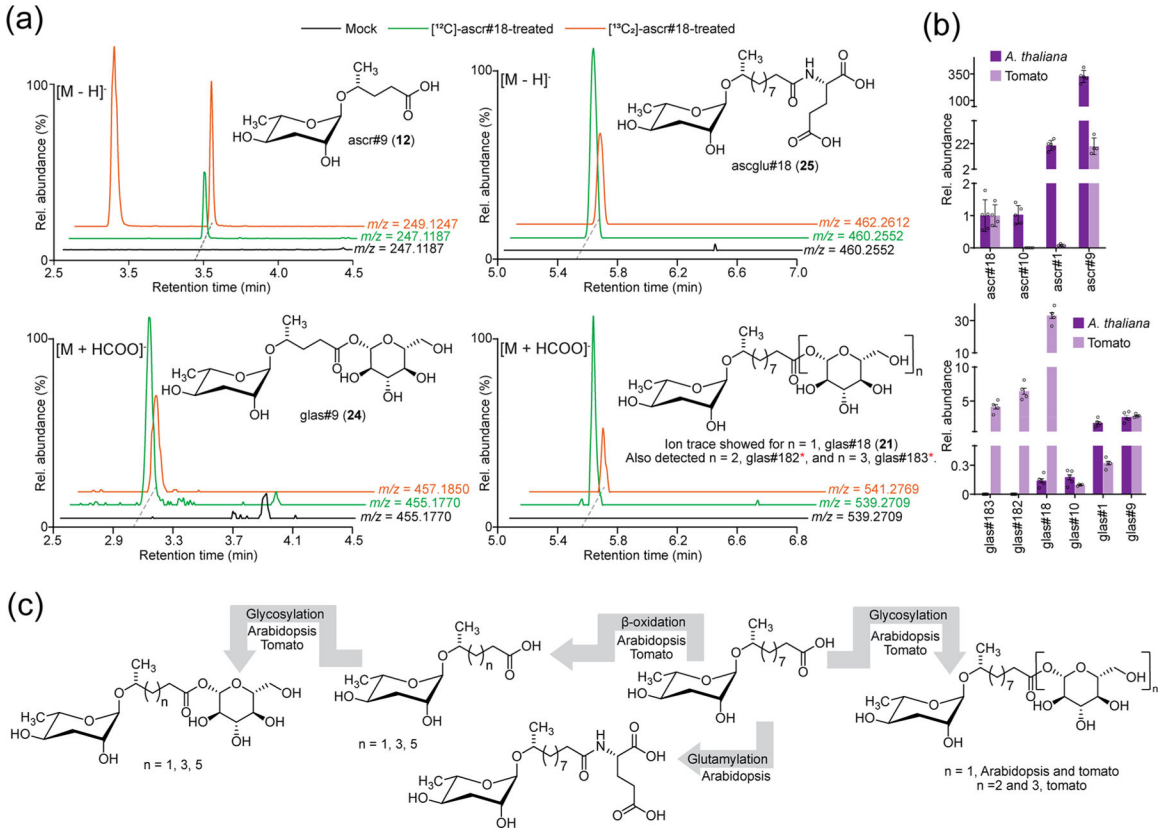

Figure 4.

ascr#18-derived metabolites from plants. (a) Example structures and ion chromatograms (ESI negative) of ascr#18 derivatives from treatment of Arabidopsis and tomato with [$^{13}C_2$]-labeled and unlabeled ascr#18. Relative differences in the abundance of [$^{13}C_2$]-labeled and unlabeled isotopomers are due to variation between experiments. (b) Abundance of ascr#18 chain-shortened metabolites (top) and glycosylated metabolites (bottom) in Arabidopsis (purple) and tomato (pink), relative to ascr#18. (c) Proposed metabolic pathways of ascr#18 in Arabidopsis and tomato. Structures of compounds marked with an asterisk (*) were proposed based on MS^2 spectra and homology with known compounds.